Gallotannin is a DNA Damaging Compound That Induces Senescence Independently of p53 and p21 in Human Colon Cancer Cells

Racha Al-Halabi,[1,2] Raghida Abou Merhi,[1] Saritha Chakilam,[3] Chirine El-Baba,[3] Eva Hamade,[1] Pietro Di Fazio,[2] Matthias Ocker,[2] Regine Schneider-Stock,[3] and Hala Gali-Muhtasib[4]*

[1]*Department of Biology, Faculty of Sciences, EDST, Lebanese University, Beirut, Lebanon*
[2]*Institute for Surgical Research, Philipps University of Marburg, Marburg, Germany*
[3]*Experimental Tumorpathology, Institut of Pathology, University of Erlangen-Nürnberg, Erlangen, Germany*
[4]*Department of Biology, American University of Beirut, Beirut, Lebanon*

The plant secondary metabolite gallotannin (GT) is the simplest hydrolyzable tannin shown to have anti-carcinogenic properties in several cell lines and to inhibit tumor development in different animal models. Here, we determined if GT induces senescence and DNA damage and investigated the involvement of p53 and p21 in this response. Using HCT116 human colon cancer cells wildtype for $p53^{+/+}$/$p21^{+/+}$ and null for $p53^{+/+}$/$p21^{-/-}$ or $p53^{-/-}$/$p21^{+/+}$, we found that GT induces senescence independently of p21 and p53. GT was found to increase the production of reactive oxygen species (ROS) by altering the redox balance in the cell, mainly by reducing the levels of glutathione and superoxide dismutase (SOD). Using the key antioxidants *N*-acetyl cysteine, dithiothreitol, SOD, and catalase, we showed that ROS were partially involved in the senescence response. Furthermore, GT-induced cell cycle arrest in S-phase in all HCT116 cell lines. At later time points, we noticed that p53 and p21 null cells escaped complete arrest and re-entered cell cycle provoking higher rates of multinucleation. The senescence induction by GT was irreversible and was accompanied by significant DNA damage as evidenced by p-H2AX staining. Our findings indicate that GT is an interesting anti colon cancer agent which warrants further study.

Key words: gallotannin; colon cancer; reactive oxygen species; anti-cancer; senescence

INTRODUCTION

Colorectal cancer is a leading cause of cancer related deaths worldwide and the third most commonly diagnosed cancer in males and females [1]. Colorectal cancer has been strongly associated with environmental causes, such as smoking, heavy alcohol use, high intake of red meat, and reduced physical activity [2,3]. Mortality associated with colon cancer could be decreased by controlling these risk factors, primarily by increasing the intake of fruits and vegetables [2–4].

Over the last decade, there has been a great deal of progress in the development of new therapies for the treatment of colorectal cancer [5,6]. Phenolic phytochemicals are among the naturally occurring substances that have shown promising anti-tumorigenic activities and low toxicity in comparison to the significant toxicity of standard chemotherapeutic agents used in the clinic today [4,7–9]. A family of polyphenols, the hydrolysable tannins, was also found to possess anti-cancer properties by inducing either growth arrest or apoptosis [10,11].

The polyphenolic hydrolyzable tannin, gallotannin (GT, Figure 1A) formed of polygalloyl esters of glucose possesses interesting anti-carcinogenic properties [12–15]. GT and penta-1,2,3,4,6-*O*-galloyl-beta-D-glucose (PGG), a precursor of GT, have been shown to exert various biological effects ranging from anti-inflammatory to anti-cancer effect in various tumor cells [16–18]. We have previously shown that GT inhibits the growth of HCT116 $p53^{+/+}$ and $p53^{-/-}$ colon cancer cells and induces cell cycle arrest in both cell lines [19]. In addition, the precursor of GT (PGG) was found to induce S-phase and G1 cell cycle arrest in breast and prostate cancer cells [20,21]. In a recent study, PGG was found to induce senescence mediated by reactive

Abbreviations: GT, gallotannin; PGG, penta-1,2,3,4,6-*O*-galloyl-beta-D-glucose; ROS, reactive oxygen species; RTCA, real time cell analysis; CI, cell index; BrdU, 5-bromo-2-deoxyuridine; pRB, retinoblastoma protein; Chk1, checkpoint 1 protein; H3, histone 3; NAC, *N*-acetyl cysteine; DTT, dithiothreitol; SOD, superoxide dismutase; CAT, catalase; GSH, glutathione; H3K9M3, trimethyl-histone H3 (lys9); SF, surviving fraction; SAHF, senescence-associated heterochromatin foci.

Conflict of interest: The authors confirm that there are no conflicts of interest.

Grant sponsor: German Academic Exchange Service (DAAD); Grant sponsor: Lebanese Research team Funds; Grant number: ER031; Grant sponsor: Lebanese University; Grant sponsor: German Deutsche Forschungsgemeinschaft

*Correspondence to: Department of Biology, American University of Beirut, PO Box 11-0236, Riad El Solh 1107 2020, Beirut, Lebanon.

Received 9 October 2013; Revised 4 April 2014; Accepted 7 April 2014

DOI 10.1002/mc.22172

Published online 6 May 2014 in Wiley Online Library (wileyonlinelibrary.com).

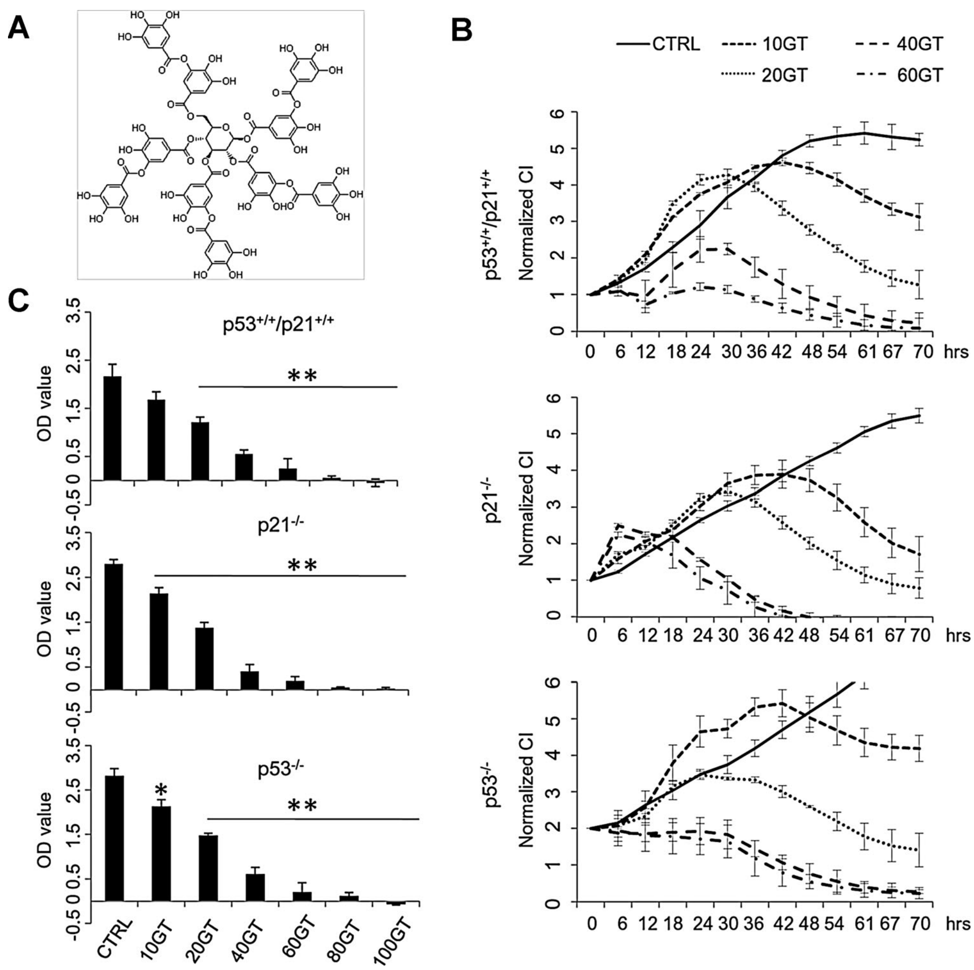

Figure 1. GT decreases cell proliferation. (A) Chemical structure of gallotannin, the simplest hydrolyzable tannin formed of polygalloyl esters of glucose. (B) HCT116 $p53^{+/+}/p21^{+/+}$, $p53^{+/+}/p21^{-/-}$, and $p53^{-/-}/p21^{+/+}$ were plated in the 96 E-plate at a density of 10^5 cells/mL. Cells were treated with 10, 20, 40, and 60 μg/mL of GT and monitored using the RTCA Xcelligence system. Displayed is the normalized CI of the start point of the treatment until 70 h. The mean and SD of triplicate measurements from one representative experiment out of three is presented. (C) HCT 116 $p53^{+/+}/p21^{+/+}$, $p53^{+/+}/p21^{-/-}$, and $p53^{-/-}/p21^{+/+}$ were plated in the 96-well plates at a density of 1.4×10^5 cells/mL. Cells were treated at 50% confluence with 10, 20, 40, 60, 80, and 100 μg/mL of GT and DNA synthesis was assessed by the BrdU incorporation ELISA kit. Each value is the mean ± SD of three separate experiments performed. $^{**}P < 0.01$, $^{*}P < 0.05$ versus control group.

oxygen species (ROS) in human breast cancer cells [22]. In vivo, GT was found to inhibit the proliferation of different types of cancer cells (breast, colon) [20,21]. GT was also shown by our group to inhibit 1,2-dimethylhydrazine (DMH)-induced colonic aberrant crypt foci [23] and tumor growth in non-obese diabetic severe combined immunodeficient mouse (NOD/SCID) mice bearing human colon cancer xenografts by inhibiting key molecular markers of cell proliferation, angiogenesis, and metastasis [24].

Cellular senescence is a state of irreversible cell cycle arrest. Senescent cells are characterized by flattened cellular morphology, the expression of β-galactosidase and senescence-associated heterochromatic foci [25,26]. The two tumor suppressor axes p53–p21 and RB-p16 are known to play critical roles in senescence [27]. Senescence can be activated in response to oncogenes; oxidative stress and DNA damage [28]. The DNA damage response is detected via the phosphorylation of H2AX, one of the earliest responses to DNA damage [29]. A recent body of evidence suggests that induction of senescence can be exploited as a basis for cancer therapy [30]. Strategies that induce senescence in cancer cells could provide future therapies complementary to existing interventions aimed at apoptosis [30,31].

Here we investigated GT effects on senescence and DNA damage in three human colon cancer HCT116 cells that differ in their p53 and p21 status. We show that GT induces senescence independent of p21 and p53 with the partial involvement of ROS in this effect. In addition, GT altered the activities of key ROS scavenging enzymes that are essential for maintaining the redox balance in the cell. Treatment with GT caused significant decrease in the ability of cells to form colonies in all three HCT116 cell lines, an effect that was irreversible. In addition, GT perturbed cell cycle progression, induced DNA damage and provoked considerable multinucleation in a p53–p21 dependent manner. These findings suggest that GT is a promising drug for colon cancer therapy. This readily available and inexpensive plant derived compound is worth further investigation for translation to the clinic.

MATERIALS AND METHODS

Cell Culture and GT Treatment

HCT116 p21$^{+/+}$/p53$^{+/+}$ human colon cancer cells were grown in RPMI 1640 with 25 mm HEPES and L-glutamine. HCT116 p53$^{+/+}$/p21$^{-/-}$ and p53$^{-/-}$/p21$^{+/+}$ cells were grown in Dulbecco's modified Eagle medium (DMEM) supplemented with sodium pyruvate and 4,500 mg/L glucose (Sigma–Aldrich, Munich, Germany). Normal human intestinal epithelial cells (FHs74Int) were cultured in Hybricare medium (ATCC, Manassas, VA). All media were supplemented with 1% penicillin–streptomycin (100 U/mL) and 10% heat-inactivated FBS (Sigma–Aldrich). Normal intestinal cells were also supplemented with 30 ng/mL of epidermal growth factor (Sigma–Aldrich). All cultured cells were grown in a humidified atmosphere of 5% CO_2 and 95% air. All cell lines were purchased from ATCC. The HCT116 p53 null cells were kindly provided by Dr. Carlos Galmarini (INSERM, Lyon, France) and the HCT116 p21$^{+/+}$/p53$^{+/+}$, p53$^{-/-}$/p21$^{+/+}$, FHs74Int, and DLD-1 were provided by Dr. Regine Schneider-Stock (Erlangen, Germany). GT (Sigma–Aldrich) was freshly dissolved in ethanol (10 mg/mL stock) and applied at different concentrations (1, 3, 9, 10, 20, 27, 40, 60, 80, 100 μg/mL) to 50% confluent cells.

Real Time Cell Analysis (RTCA)

Cells were plated in the E-Plate 96-microwell at a density of 1×10^5 cells/mL. Cell attachment spreading and proliferation were continuously monitored using the xCELLigence System (RTCA MP, Roche, Mannheim, Germany). Cell-free medium was used as reference to measure the background impedance for calculating cell index (CI). The CI was measured every 30 min for 24 h before treatment with different concentrations of GT (10, 20, 40, and 60 μg/mL). CI was measured again every 15 min after treatment up to 70 h. All CIs were normalized to the time of treatment which was considered as $t = 0$.

Cell Proliferation ELISA BrdU

Cells were plated in 96-well plates at a density of 1.4×10^5 cells/mL in a final volume of 100 μL culture medium per well. The 5-bromo-2-deoxyuridine (BrdU) incorporation assay was carried out using the Cell Proliferation ELISA kit according to the manufacturer's guidelines (Roche). Cells were treated with 10, 20, 40, 60, 80, and 100 μg/mL of GT and incubated for 48 h. BrdU labeling solution was added to a final concentration of 10 μM, and cells incubated for an additional 4 h at 37°C. Incorporated BrdU was detected using anti-BrdU-POD, and sample absorbance was measured at 405 nm against background control (reference wavelength: 690 nm), using a Victor 3 multiwell plate reader (PerkinElmer, Waltham, MA).

Senescence Associated β-galactosidase Activity

HCT116 cells were plated in six-well tissue culture dishes at a density of 1.4×10^5 cells/mL. Cells were treated with 20 and 60 μg/mL GT and incubated for 48 h. After the treatment, cells were fixed with a fixative solution and stained with a staining solution provided by the kit (Sigma–Aldrich). The cells were then incubated overnight at 37°C. Cells were checked under the microscope, at 20× magnification, for the development of blue color (Axiovert 200, Zeiss, Göttingen, Germany). For quantification of senescent cells, the percentage of senescing cells for each sample was determined by calculating the average number of senescing cells in five random regions.

Protein Extraction and Immunoblot Analysis

Cells were plated in six-well plates at a density of 1.4×10^5 cells/mL and were treated with 20, 40, and 60 μg/mL concentration of GT. Protein extracts were prepared using urea buffer (4 M urea, 0.5% SDS, 62.5 mM tris, 4% protease inhibitors, and 1% phosphatase inhibitors). Proteins were quantified by DC BioRad protein assay kit (BioRad, Munchen, Germany). Fifty microgram of whole cell lysate was separated by SDS–PAGE (12% gels) and transferred to nitrocellulose membranes (Amersham Pharmacia Biotech, Little Chalfont, UK). The membranes were probed with the primary antibodies p53 (Santa Cruz, sc-6243, Santa Cruz, CA), p21 (Cell Signaling, 2946, Boston, MA), retinoblastoma protein (pRB) (Biosource, Hercules, CA), Cyclin B_1 (Santa Cruz, sc-752), Cyclin D1 (Cell Signaling, 2922), checkpoint 1 protein (chk1) (Santa Cruz, SC-8408), pchk1 (Abcam, AB-2834, Cambridge, MA), histone 3 (H3) (Active motif, 39163, Carlsbad, CA), pH3 (Cell Signaling, 9701), cdc2 (Cell Signaling, 9112), pcdc2 (Cell Signaling, 2543), p-H2AX (Merck Millipore, 05-636, Darmstadt, Germany) followed by horseradish peroxidase-conjugated anti-mouse, anti-rabbit, or anti-goat IgG-HRP (Santa Cruz). GAPDH was used to ensure equal protein loading. The immunoreactive bands were detected with enhanced chemiluminescence system (ECL) (Roche).

Immunofluorescence Staining

Cells were plated at 1.4×10^5 cells/mL on glass coverslips in six-well plates and treated with 20 μg/mL for 48 h. Cells were fixed using 70% ethanol. Fixed cells were blocked and permeabilized for 1 h in PBS and 3% normal goat serum (NGS) (Santa Cruz). Primary antibodies p-H2AX (Merck Millipore, 05-636), anti-trimethyl-histone H3 (lys9) (Upstate Millipore, 07-442, Billerica, MA), phalloidin-Alexa488 (Invitrogen, A12379, Carlsbad, CA) were diluted in PBS and incubated on the cells for 2 h. Afterwards, the cells were washed with PBS and incubated for 1 h with the appropriate secondary fluorescein anti-rabbit IgG (Molecular Probes, Eugene, OR) after which they were counterstained with Hoechst (Invitrogen). F-actin filament staining with phalloidin coupled with AlexaFluor was directly counterstained with Dapi (Invitrogen) for nuclear staining. The slides were then mounted on microscope slides using one drop of FluorSaveTM reagent (Calbiochem, Darmstadt, Germany). Images were taken with the fluorescent microscope (Axiovert 200, Zeiss).

Cell Cycle Analysis Using Flow Cytometry

Cells were plated in six-well plates at a density of 1.4×10^5 cells/mL. Cells were treated with 20 μg/mL of GT and incubated for 48 h. Supernatants containing the dead cells were collected and attached live cells were harvested by trypsinization. The cells were then fixed with 70% ice-cold ethanol. After washing the cells were incubated with 200 μg/mL RNase A (Roche) for 1 h at 37°C. Cells were then washed with 1× PBS and stained with 100 μg/mL of propidium iodide (Invitrogen). The cellular fluorescence was measured by flow cytometry using a fluorescence activated cell sorter (FACS) flow cytometer (Becton Dickinson, Franklin Lakes, NJ). Cell Quest program was used to determine the percentages of cells in various cell cycle phases. Pre-G1 cells with DNA content $<2n$ represent apoptotic or necrotic cells.

Colony Formation Assay

The soft agar colony formation assay was used to assess the anti-tumorigenic activity of GT in vitro. The assay was performed in six-well tissue culture dishes containing two layers of agarose. Bottom layer was prepared with 1.5 mL of complete RPMI/DMEM medium supplemented with 0.5% agarose (Sigma–Aldrich), 5×10^5 single cells were resuspended in 1.5 mL of corresponding medium supplemented with 0.35% agarose and overlaid on the bottom layer. Thereafter, cells were cultured in the presence or absence of GT (40 μg/mL) for 14 days. The medium was replenished on every third day. After 2 weeks of incubation period, the colonies were stained with crystal violet (0.005%) (Carl Roth, Karlsruhe, Germany), counted, and imaged by microscopy (Axiovert 200, Zeiss).

Clonogenic Survival Assay

Cells were treated with GT (1, 3, 9, 20, 27, 40, and 60 μg/mL) for 48 h after which they were trypsinized, and replated at low densities (1,000 cells) in T-25 flasks, and left for 14 days in the incubator. The cells were replenished with fresh media after 5 days in culture and afterwards new media was added every 2 days. Subsequently, cells were washed with PBS, and stained with crystal violet (0.5%). Colonies having more than 50 cells were counted. The plating efficiency (PE), defined as the ability of control cells to survive and grow into colonies, was calculated as follows: PE = colonies counted in control/plating density of control. Surviving fraction (SF) for each treatment was calculated according to the following formula: SF = colonies counted/[cells plated × (PE/100)] [32]. The SF value of each treatment was then plotted.

Intracellular ROS Detection by DCFH

Cells were plated in six-well plates at a density of 1.4×10^5 cells/mL and treated in media containing 2% FBS without or with 20, 40, or 60 μg/mL GT for 10 min. The cells were pre-treated for 2 h with 2 mM of *N*-acetyl cysteine (NAC) (Sigma–Aldrich). 2′,7′-Dichlorodihydrofluorescein diacetate (DCFH-DA) was used to measure the ROS level. This molecule passively diffuses into the cells and is cleaved and oxidized in the intracellular environment to the green fluorescence emitting compound, 2′,7′-dichlorofluorescein (DCF). Attached cells were harvested, washed, and incubated with 10 μM H2DCFDA (Invitrogen) for 20 min at 37°C. Cells were washed, resuspended in PBS and ROS generation was determined by flow cytometric analysis on the FL-1 channel (Becton Dickinson).

Measurements of Antioxidant Enzymes Activities

Antioxidant enzyme levels were measured using the following kits: superoxide dismutase (SOD) was measured using SOD Assay Kit (BioVision, Milpitas, CA); catalase (CAT) was performed using CAT assay Kit (BioVision) and glutathione (GSH) was determined using the GSH assay (Oxford Biomedical Research, Rochester Hills, MI). Cells were treated with 20 μg/mL GT for 15 min and the samples were processed according to manufacturer's instructions. Relative antioxidant levels (CAT, SOD, and GSH) were normalized by protein amount and are represented as the ratio to 100%, which is the respective antioxidant activity in control cells.

p-H2AX Detection by Flow Cytometry

As an early sensor for DNA damage response, the phosphorylated H2AX (p-H2AX), was detected by flow cytometry. Cells were collected and fixed with ice-cold 70% ethanol. Cells were washed and permeabilized with the buffer BSA-T-PBS containing 1% BSA and 0.2% Triton X-100 dissolved in 1× PBS for 10 min on ice. Next the cells were suspended in BSA-T-PBS containing the primary antibody p-H2AX (Merck Millipore) at a dilution of 1:100, and incubated overnight at 4°C. Afterward the cells were washed twice with BSA-T-PBS, and the pellets were then incubated in the dark with the fluorescein isothiocyanate (FITC)-conjugated secondary anti-mouse antibody (Cell Signaling) for 1 h at room temperature. After washing with BSA-T-PBS, cells were resuspended in TBS and analyzed using the flow cytometer (Becton Dickinson).

Experiments with NAC were performed using the p-H2AX staining kit (Upstate Millipore). The cells were pre-treated for 2 h with 2 mM NAC (Sigma–Aldrich) followed by 48 h of 20 μg/mL of GT. Cells were stained according to the manufacturer's instructions, and p-H2AX levels were measured by flow cytometry.

Statistical Analysis

Statistical analysis was performed on raw data using SPSS v16.0. One-way analysis of variance (ANOVA) followed by Tukey's and Duncan's multiple range test was used to compare multiple treated samples versus a single sample while a one-tailed *t*-test was used to compare any significant difference between any two samples. Statistical significance was assumed when the *P*-value was less than 0.05.

RESULTS

Gallotannin Decreases Cell Proliferation and DNA Synthesis

Previously, we have reported that GT induces a differential p53-dependent apoptotic effect in HCT116 colon cancer cell lines [19]. Therefore, in this study three HCT116 colon cancer cell lines, wildtype for $p53^{+/+}/p21^{+/+}$, and knock out for p21 ($p53^{+/+}/p21^{-/-}$) or p53 ($p53^{-/-}/p21^{+/+}$) were used as a model to investigate GT effects on cell proliferation and cell cycle regulation. The real time cell analysis (RTCA) measures the CI which can be used to monitor cell proliferation, viability, and cytotoxicity [33,34]. Using the RTCA system we examined the effect of different concentrations of GT (10, 20, 40, and 60 μg/mL) on the CI of the three HCT116 cell lines for up to 70 h. Treatment with GT resulted in a time- and dose-dependent decrease in CI, corresponding to the inhibition of cell viability and proliferation (Figure 1B). In each of the three HCT116 cell lines, GT induced a different kinetic profile as described by the manufacturer [35]. In $p53^{+/+}/p21^{+/+}$ cells, the profile was that of a cytotoxic effect, while in the $p53^{+/+}/p21^{-/-}$ cells it was anti-mitotic and a cytostatic profile was observed in the $p53^{-/-}/p21^{+/+}$ cells (Figure 1B). Higher concentrations of GT (40 and 60 μg/mL) caused significant inhibition of CI by 48 h, whereas at lower concentrations (10 and 20 μg/mL), we observed an accelerated increase of the normalized CI as compared to control which can be interpreted as a sign of drug-induced senescence (Figure 1B).

We also evaluated the effect of GT on cell proliferation by measuring BrdU incorporation. GT inhibited BrdU incorporation after 48 h especially at the highest concentration of 100 μg/mL (Figure 1C). After 48 h of 20 μg/mL GT, the $p53^{+/+}/p21^{+/+}$ cells had an absorbance of 1.2 and similar findings were observed in the $p53^{+/+}/p21^{-/-}$ (OD = 1.3) and $p53^{-/-}/p21^{+/+}$ (OD = 1.4) cell lines. Thus, GT caused more than 50% decrease in BrdU incorporation which is indicative of significant reduction in proliferation (Figure 1C).

Senescence Induction Potential of Gallotannin

In order to investigate if the inhibition of proliferation in response to GT is due to senescence, we assayed senescence induction 48 h post-treatment using the senescence β-galactosidase staining kit. Treatment with 20 μg/mL GT for 48 h increased the number of β-galactosidase stained cells in all three HCT116 cell lines (Figure 2A). At 20 μg/mL GT the percentage of β-galactosidase positive cells increased by 43–45% in all three cell lines compared to the control (Figure 2A, left panel). However, higher concentrations of GT (40 and 60 μg/mL) did not show any signs of senescence (Figure S1A). The similar increase in β-galactosidase positive cells in response to 20 μg/mL GT in all three cell lines suggested that the presence or absence of p53 or p21 does not affect GT-induced senescence. Interestingly, β-galactosidose staining in the FHs74Int normal human intestinal epithelial cells indicated no signs of senescence after GT treatment (Figure S1B) reconfirming the selective toxicity of GT to colon cancer cells.

To investigate whether senescence is a generalized effect induced by GT in other colon cancer cell lines, we determined the β-galactosidase activity in the human colon cancer DLD1 cells ($p53^{+/+}$) [36,37]. Cells were treated with 20 μg/mL GT for 48 h after which they were stained for senescence-associated β-galactosidase activity. GT was also found to increase the formation of blue colored cells in DLD1 indicative of senescence (Figure S1C).

The formation of senescence-associated heterochromatin foci (SAHFs) which are transcriptionally silent regions of DNA is known to enforce cellular senescence by repressing genes involved in cell proliferation [38–40]. HCT116 cell lines were treated with GT and stained with Hoechst as well as the trimethylated form of Lys 9 on histone H3 (H3K9m3) antibody, a specific component of the heterochromatic SAHF [40]. The formation of SAHF foci were observed in all three cell lines after 48 h in response to 20 μg/mL GT. A partial co-localization of Hoechst stained heterochromatin foci with H3K9m3 was observed compared to a diffuse nuclear pattern in the control (Figure 2B).

Modulations in the expression levels of proteins of the p53–p21 pathway as well as the RB protein which are known to play an important role in cell cycle arrest and senescence induction were investigated [27]. The hypophosphorylated form of RB is known to activate senescence in many cell models [28]. HCT116 cell lines were treated with 20 μg/mL GT and whole cell

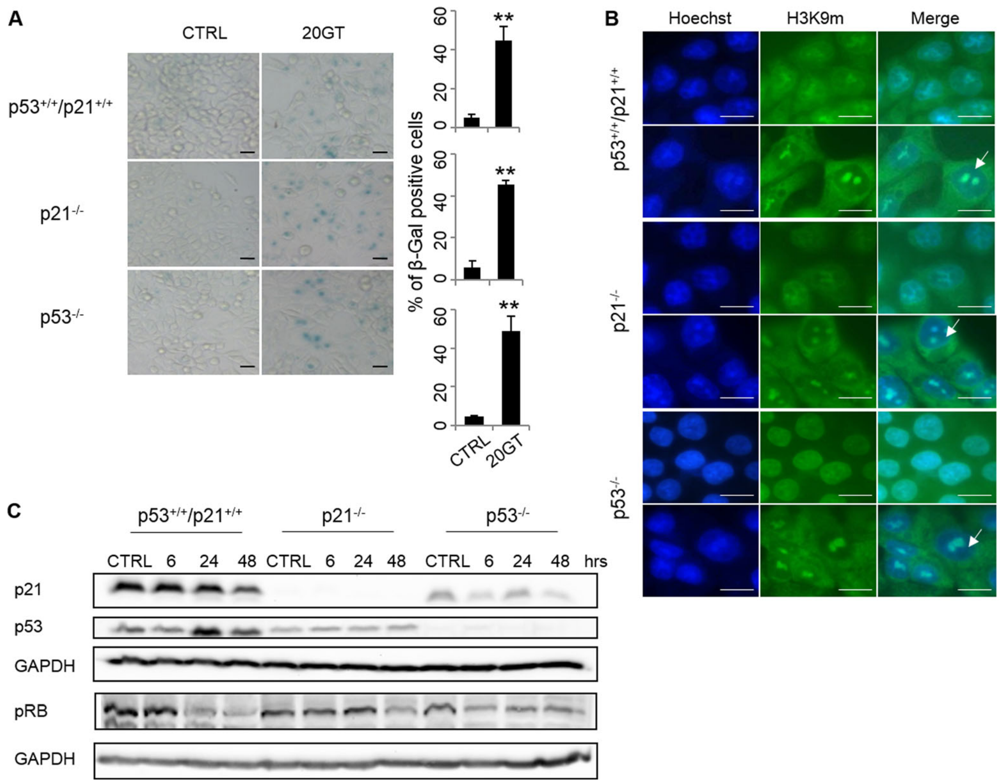

Figure 2. GT treatment induces senescence in all three HCT116 cell lines. (A) Cells were treated with 20 μg/mL GT for 48 h. Senescence induction was assayed by the Senescence β-galactosidase Staining kit as described in the Materials and Methods section. Stained cells were viewed and 5 pictures/condition were taken under an inverted microscope at 20× for quantitative analysis. The pictures are representative of three independent experiments. Scale bar: 20 μm. $^{**}P < 0.01$ versus control group. (B) HCT116 cells were treated with 20GT for 48 h. The cells were co-stained with H3K9m3 (green) and Hoechst (blue) to detect senescence-associated heterochromatin foci (SAHF) formation. Images were taken by a fluorescent microscope at 100× magnification. Scale bar, 10 μm. The pictures are representative of two independent experiments. (C) The HCT116 $p53^{+/+}/p21^{+/+}$, $p53^{+/+}/p21^{-/-}$, and $p53^{-/-}/p21^{+/+}$ were treated with 20 μg/mL GT for 6, 24, and 48 h. Whole cell lysate were immunoblotted for p21, p53, and pRB antibodies. The membranes were also probed with GAPDH antibody to ensure equal loading. The blots are representative of three independent experiments.

extracts were prepared after 6, 24, and 48 h of treatment. The modulation of p53 was screened by western blot analysis in $p53^{+/+}/p21^{+/+}$ HCT116 and $p53^{+/+}/p21^{-/-}$cells. In $p53^{+/+}/p21^{+/+}$ cells, GT treatment caused a significant increase in p53 protein expression especially after 24 h at 20 μg/mL GT (Figure 2C). Whereas, the expression of the cyclin dependent kinase inhibitor p21, a major downstream effector of p53, was not sustained after 24 and 48 h of GT treatment (Figure 2C), suggesting that this phenomenon is mediated by some p53 and p21 independent pathways. As expected, GT treatment was found to inhibit the protein expression levels of pRB time-dependently in all three HCT116 cell lines (Figure 2C). The protein expression results together with the β-galactosidase and SAHF findings confirmed the lack of involvement of p21 and p53 in GT-induced senescence.

Gallotannin Disrupts Cell Cycle Progression and Induces p53–p21 Dependent Multinucleation

In order to investigate if GT-induced senescence is associated with cell cycle changes, we analyzed the effect of GT on cell cycle distribution by propidium iodide staining of DNA content. Upon treatment with 20 μg/mL GT for 24 and 48 h, all three cell lines showed a decrease in the G1 population concomitant with the accumulation of cells in the S phase, suggesting S phase arrest (Figure 3A). Although the extent of S phase arrest was similar in the three cell lines, yet, the percentage of cells in SubG1, representing the population of dead cells, increased to a greater extent in p53 and p21 null cells in comparison to cells with intact p53 and p21, suggesting that the absence of the damage sensor p53 or its major target p21 commits the cells to death. To correlate the alterations in cell cycle progression with changes in molecular markers, we evaluated GT effects on key cell-cycle regulatory proteins and mitotic markers by western blot (Figure 3B). We could distinguish a clear difference in the response of the three cell lines after early (6 h) and late (24–48 h) times of incubation with GT. At early times, we observed an increased expression of cyclin B1/cyclin D1 in GT treated cells in comparison to the control, namely in the $p53^{+/+}$ cell line (Figure 3B). This suggests that GT prompts an early push of the cells through the cell cycle in

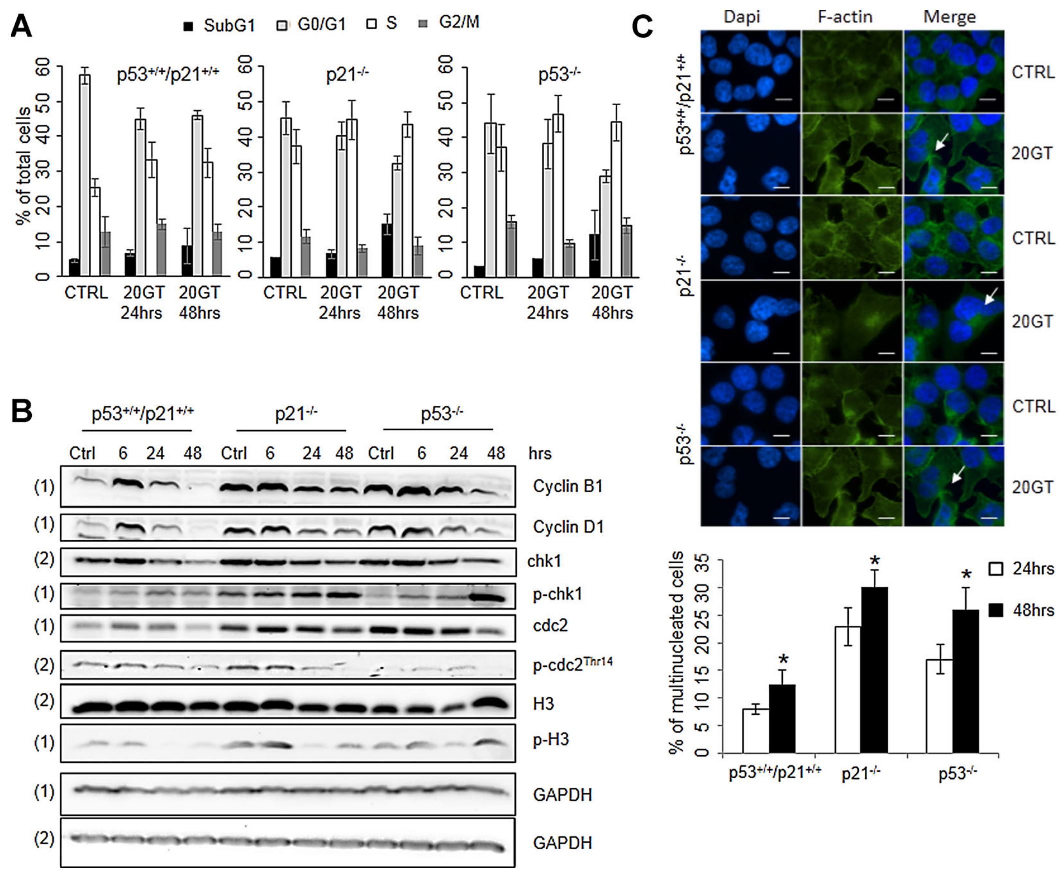

Figure 3. GT impairs cell cycle and induces multi nucleation in a p53–p21 dependent manner. (A) Cells were treated with GT 20 μg/mL for 24 and 48 h. Cells were then harvested and DNA was stained with PI for flow cytometric analysis of DNA content with FACScan flow cytometry. The percentage of cells in each of the cell cycle phases was calculated using Cell Quest. Each value is the mean of three separate experiments. (B) The HCT116 $p53^{+/+}/p21^{+/+}$, $p53^{+/+}/p21^{-/-}$, and $p53^{-/-}/p21^{+/+}$ were treated with 20 μg/mL GT for different time points (6, 24, and 48 h). Whole cell lysate were immunobloted for Cyclin B1, Cyclin D1, chk1, pchk1, cdc2, pcdc2, H3, and pH3. GAPDH was used to ensure equal loading [GAPDH (1) corresponds to loading control for cyclin B1, cyclin D1, pchk1, cdc2, and pH3; GAPDH (2) corresponds to chk1, pcdc2, and H3)]. The blots are representative of three independent experiments. (C) HCT116 cells $p53^{+/+}/p21^{+/+}$, $p53^{+/+}/p21^{-/-}$, and $p53^{-/-}/p21^{+/+}$ were treated with 20 μg/mL GT for 24 and 48 h. The cells were co stained with Phalloidin staining for F-actin (green) and dapi (blue) and images were taken and quantified by fluorescent microscope at 100× magnification. The pictures are representative of three independent experiments. Scale bar: 10 μm. For each condition, 100 cells randomly chosen from different views were scored for multinucleated cells. Each value is the mean ± SD of three separate experiments. $^*P < 0.05$ versus 24 h treated group.

HCT116 $p53^{+/+}/p21^{+/+}$cells. The three cell lines differed significantly in their molecular response to GT at later times of incubation (especially at 48 h) which was dependent on the p53 and p21 cellular status. In $p53^{+/+}/p21^{+/+}$ cells, GT abolished completely the expression levels of cyclin B1, cyclin D1, and pH3 consistent with a simultaneous blockage in cell progression at all phases of the cell cycle. Interestingly, this block in response to GT in $p53^{+/+}/p21^{+/+}$ cells resulted in the lowest level (12%) of multinucleation observed in this cell line (Figure 3C). GT treatment in p53 and p21 deficient cells resulted in more SubG1 dead cells concomitant with the highest increase in the expression levels of the damage sensor pchk1, while this protein was not induced in the $p53^{+/+}/p21^{+/+}$cells (Figure 3B). In contrast, cells deficient for p53 and p21 were able to escape complete arrest and re-enter the cell cycle, which is evidenced by a further reduction in the G1 population (Figure 3A), the retrieval of pH3 expression and the steady state level of cyclin B1 (Figure 3B). This re-entry of damaged cells into cell cycle could be responsible for the increased multinucleation (28%) in these two cell lines in comparison to the $p53^{+/+}/p21^{+/+}$ cells (Figure 3C). The increased multinucleation in cells deficient for p53 and p21 was further confirmed by quantifying the >4N population by flow cytometry (data not shown). This degree of GT-induced multinucleation in cells that lack p53 and p21 (Figure 3C) correlates well with the relatively higher levels of cell death observed in these cell lines (Figure 3A). These results indicate that GT blocks cell cycle progression mostly in HCT116 cells with intact p53/p21 and causes cell death and multinucleation foremost in the null cell lines. Moreover, $p53^{-/-}/p21^{+/+}$ and $p53^{+/+}/p21^{-/-}$ cells also showed a higher percentage of senescent cells (12%) that are also multinucleated in comparison to the $p53^{+/+}/p21^{+/+}$ cells (5%).

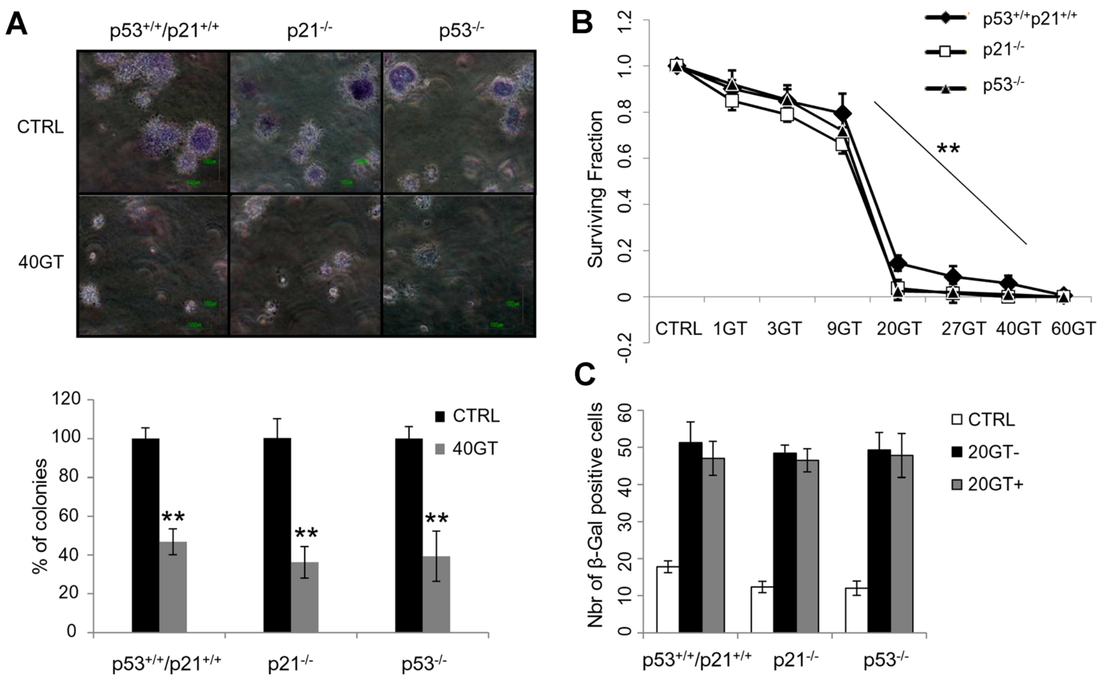

Figure 4. GT effect is irreversible in HCT116 cells. (A) Clonogenic assay on gel agar, cells were cultured in the presence or absence of gallotannin (40 μg/mL) for 14 days. After 2 weeks of incubation period, the colonies were stained with crystal violet (0.005%), counted, and imaged by phase-contrast light microscopy. The data represent the mean ± SD of three independent experiments. $^{**}P < 0.01$ versus control group. (B) The cells were treated with different concentrations of GT (1, 3, 9, 20, 27, 40, and 60 μg/mL) for 48 h. Cells were replated at low density and colonies having more than 50 cells were counted after 14 days. Surviving fractions were calculated as mentioned in the Materials and Methods section. The data represent the mean ± SD of three independent experiments. $^{**}P < 0.01$ versus control group. (C) HCT116 $p53^{+/+}/p21^{+/+}$, $p53^{+/+}/p21^{-/-}$, $p53^{-/-}/p21^{+/+}$ cells were treated with 20GT for 48 h, followed by 48 h of washout in GT-free medium (20GT−) before cells were stained for β-galactosidase activity or directly stained for β-galactosidase activity after GT treatment (20GT+). Each value is the mean ± SD of three separate experiments. $^{**}P < 0.01$, $^{*}P < 0.05$ versus control group.

Gallotannin Effects on HCT116 Cells Are Irreversible

To study the anti-tumorigenic effect of GT on HCT116 cells, we investigated whether GT inhibits colony formation of HCT116 cells in soft agar, a hallmark of malignant transformation. HCT116 cells spontaneously form colonies in soft agar, independent of tumor promoters.

Cells were cultured in the presence or absence of GT (40 μg/mL) for 14 days, after which the colonies were stained with crystal violet and counted. GT significantly decreased more than half of the ability of cells to form colonies in all three cell lines (Figure 4A), suggesting that GT has anti-tumor activities by inhibiting anchorage-independent cell growth. In another long-term survival assay, cells were treated with different concentrations of GT (1, 3, 9, 20, 27, 40, and 60 μg/mL) for 48 h then replated at low density (1,000 cells) and the number of colonies was counted after 14 days in culture. The extent of inhibition of colony survival by GT was similar in the three HCT116 cell lines; 40% inhibition occurred at concentrations up to 9 μg/mL GT and almost complete inhibition was observed at 20 μg/mL GT (Figure 4B). We tested the irreversibility of GT-induced senescence after GT withdrawal. HCT116 cells were treated with 20 μg/mL GT for 48 h after which the drug was removed and cells were stained for senescence associated β-galactosidase activity after 48 h. The washout of GT did not reduce the number of senescent cells (Figure 4C), suggesting permanent and irreversible long-term effects of GT.

ROS Are Partially Responsible for Gallotannin-Induced Senescence

To determine the mechanism of senescence induction by GT, we examined two main senescence effectors namely ROS generation and DNA damage.

One of the main mechanisms of cell death by chemotherapeutic agents is the production of ROS in cancer cells [41]. Over the last decades, many experiments have validated the link between oxidants and senescence [42]. In addition, conditions that induce senescence often appear to be accompanied by a rise in intracellular ROS levels [42]. We sought to explore whether GT-induced senescence is correlated with its ability to increase ROS production by two approaches: (1) determining ROS levels in the cell after GT treatment using the DCFH assay, and (2) determining the levels of the main antioxidants in the cell [CAT, SOD, and GSH] in response to GT in addition to correlating these levels with senescence induced by GT. For ROS production, the three HCT116 cell lines were treated with 20, 40 or 60 μg/mL of GT for 10 min and incubated for 20 min with the dye H2DCFDA. We

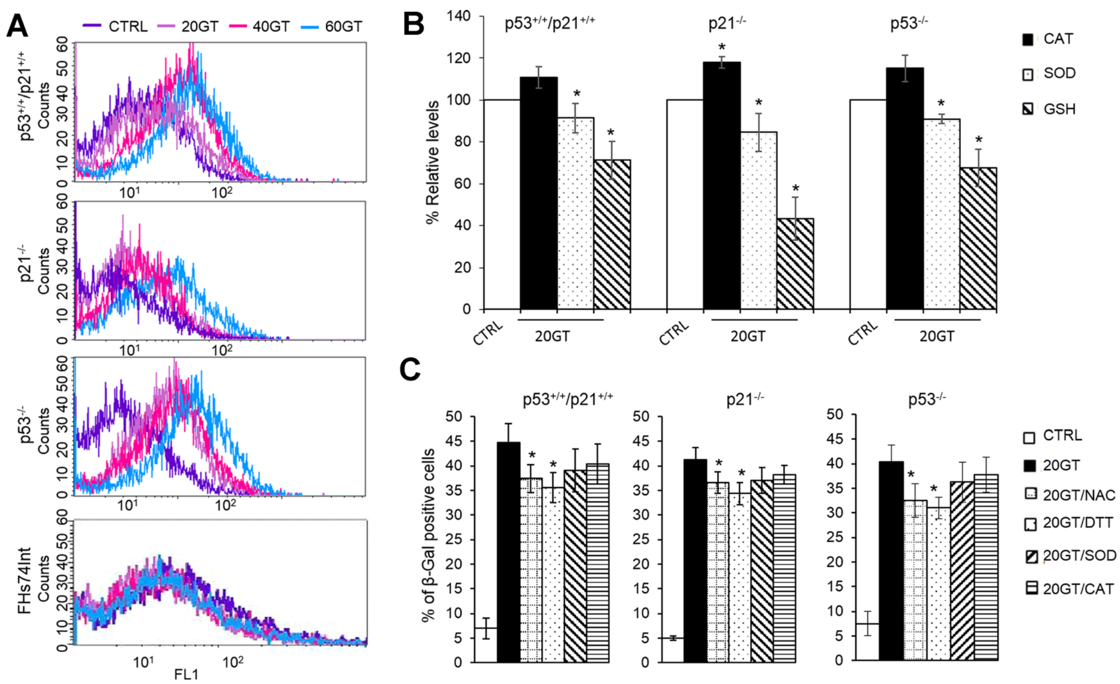

Figure 5. ROS production is partially responsible for GT-induced senescence. (A) HCT116 $p53^{+/+}/p21^{+/+}$, $p53^{+/+}/p21^{-/-}$, $p53^{-/-}/p21^{+/+}$, and normal intestinal cells (FHs74Int) were treated with 20, 40, and 60 μg/mL of GT. Cells were incubated with 10 μM H2DCFDA dye for 20 min followed with 10 min incubation with GT and fluorescence was read using flow cytometry. These results are representative of three separate experiments. (B) HCT116 cells were treated with 20 μg/mL of GT for 15 min followed by CAT, SOD, and GSH measurement. Each value is the mean ± SD of three separate experiments. $^{*}P < 0.05$ significant difference with respect to control alone. (C) HCT116 cells were treated with 20GT alone, pre-treated with 2 mM NAC 2 h before GT treatment and with 1 mM DTT, 2 mM CAT, 2 mM SOD 15 min before GT. The cells were stained for β-galactosidase activity and the cells were viewed and photographed under the microscope. Quantitative analysis of β-galactosidase positive cells was done. Each value is the mean ± SD of three separate experiments. $^{*}P < 0.05$ significant difference with respect to GT alone.

observed a dose-dependent increase in ROS production in all cell lines as measured by flow cytometry (Figure 5A). Interestingly, GT did not increase the generation of ROS in the FHs74Int normal intestinal cell line, suggesting its selectivity to cancer cells [19]. For measuring antioxidant enzyme levels, cells were treated with 20 μg/mL GT and the levels of CAT, SOD, and GSH were measured spectrophotometrically (Figure 5B). Although the levels of CAT increased in response to GT in all three HCT116 cell lines, both SOD and GSH levels decreased significantly with a more pronounced decrease observed in GSH levels (Figure 5B). These results are consistent with the increase of oxidative stress after GT treatment (Figure 5A) and indicate that GT induces a shift in the redox balance of the cell. Furthermore, we also investigated whether the antioxidants are involved in scavenging ROS production induced by GT.

To investigate whether ROS generated by GT are responsible for GT-induced senescence, we pre-treated cells with the antioxidants [2 mM NAC, 1 mM dithiothreitol (DTT), 2 mM SOD, 2 mM CAT] followed by 20 μg/mL of GT for 48 h, after which the cells were stained for β-galactosidase activity (Figure 5C). Interestingly, the potent thiol antioxidants, NAC and DTT, inhibited ROS production in response to GT to a larger extent than the enzymatic antioxidants SOD and CAT (Figure S2). Accordingly, the percentage of β-galactosidase staining decreased in cells pre-treated with NAC and DTT to a greater extent than SOD and CAT (Figure 5C), suggesting that ROS generated by GT play a role in GT-induced senescence. The lack of total reversal of the senescence phenotype in cells treated with GT and the key ROS scavenging antioxidants indicates that factors other than ROS are also responsible for GT-induced senescence.

Gallotannin Induces DNA Damage

DNA damage inducing drugs are known to cause senescence of tumor cells, a phenomenon termed drug-induced senescence, which may be exploited for the treatment of cancer [40]. Therefore, we studied the effect of GT on DNA integrity. p-H2AX staining is also known as a marker for senescence-associated DNA damage [43,44]. We treated HCT116 cell lines with 20 or 60 μg/mL of GT for 48 h and examined the formation of p-H2AX foci. The cells were co-stained with Hoechst and p-H2AX and analyzed by a fluorescence microscope. The DNA damage foci were detected in all three cell lines after GT treatment but were much more pronounced at 60 μg/mL GT (Figure 6A, left panel). We also investigated the protein expression of the p-H2AX and in accordance

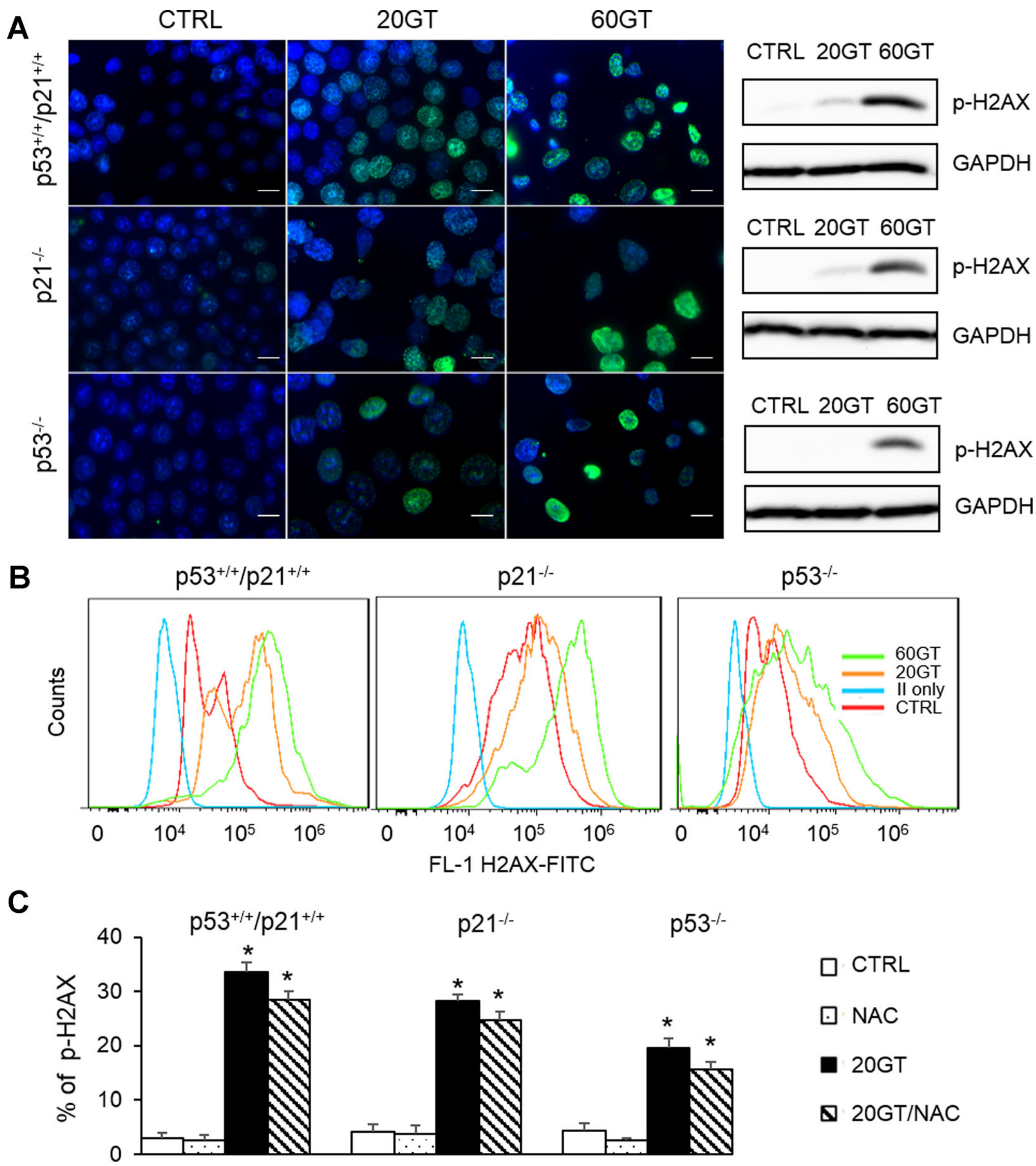

Figure 6. GT treatment causes DNA damage. (A) pH2AX (green) and Hoechst (blue) co-staining (left panel) and p-H2AX protein expression (right panel) in HCT116 cell lines treated for 48 h with 20 and 60 μg/mL GT. Images were taken by a fluorescent microscope at 100× magnification, scale bar 10 μm. Total cell protein lysates of the following conditions were immunoblotted with p-H2AX antibody and β-actin was used to ensure equal loading. The pictures and blots are representative of three independent experiments. (B) HCT116 wt, $p53^{+/+}/p21^{-/-}$, and $p53^{-/-}/p21^{+/+}$ cells were treated with 20 or 60 μg/mL GT for 48 h. Cells were fixed and stained for p-H2AX coupled with a fluorescein secondary and its expression was measured by flow cytometry. (C) Quantitative expression of p-H2AX after GT treatment. HCT116 wt, $p53^{+/+}/p21^{-/-}$, and $p53^{-/-}/p21^{+/+}$ cells were treated with 20 μg/mL GT for 48 h in the presence or absence of NAC. The percentage of p-H2AX positive cells was calculated using Cell Quest. Each value is the mean ± SD of three separate experiments performed in duplicates. $^*P < 0.01$ versus control group.

with the immunofluorescence results there was a dose dependent increase in the expression of p-H2AX indicating the activation of the DNA damage response after GT (Figure 6A, right panel).

To further confirm the DNA damage effect of GT, HCT116 cell lines were treated with 20 or 60 μg/mL GT for 48 h after which cells were stained with the p-H2AX antibody coupled with a fluorescent secondary then quantified by the flow cytometer. We observed an increase in the percentage of p-H2AX in all three HCT116 cell lines, especially at 60 μg/mL GT (Figure 6B), confirming the DNA damaging potential of GT in the three cell lines especially at the 60 μg/mL higher concentration. To investigate the role of ROS in DNA damage induced by GT, cells were pre-treated with NAC and the percentage of p-H2AX was measured by flow cytometry (Figure 6C). In all three HCT116 cells, NAC protected from p-H2AX accumulation to a limited extent, suggesting that ROS are not solely responsible for GT-induced DNA damage.

DISCUSSION

We have previously reported that GT induces apoptosis in human colon cancer HCT116 cell lines at concentrations higher than 40 μg/mL [19]. Here, we show that low concentrations of GT induce senescence, an effect which is irreversible and which is partly mediated by ROS. Our results implicate the disengagement of the p53–p21 axis in this senescence response since all three isogenic HCT116 cell lines underwent senescence with identical frequency. We also show that GT alters the activity of key ROS scavenging enzymes in the cell and is a DNA damaging drug that decreases cell proliferation and induces S-phase arrest in HCT116 cells. However, we show that prolonged GT treatment triggered, in addition to senescence, inappropriate cell cycle re-entry generating multinucleated cells especially in cells lacking p53 and p21.

Senescence is a state of irreversible cell cycle arrest in which senescent cells exhibit characteristic features such as flattened cellular morphology, and SAHF [26]. Our study showed that 20 μg/mL GT was capable of inducing senescence, as manifested by the increase of the senescence-associated β-galactosidase activity, the most commonly used marker for senescence. These results are consistent with the recent finding showing a senescence inducing effect of the naturally occurring GT PGG on hepatoma and breast cancer cells [22]. In addition, similar levels of SAHF staining occurred in all three HCT116 cell lines despite differences in their p53 and p21 status. These morphological and biochemical changes support the senescence induction potential of GT in HCT116 cells where p53 and p21 are not required for the senescence process.

Although the p53–p21 pathway has been described to be crucial for senescence induction, our results extend more evidence of the uncoupling of this axis to drug-induced senescence [22,27]. Despite the sustained induction of p53 protein in HCT116 cells upon GT treatment, p21 protein levels slightly increased at 3 h in response to low doses of GT and unexpectedly decreased at 48 h. This decrease in p21 expression might be a mechanism for allowing DNA repair to occur since high levels of p21 inhibit certain DNA repair molecules [45,46]. Many studies have highlighted that the wildtype expression of p53 and p21 is not required for senescence and that elevated expression of p21 is not a prerequisite for cellular senescence [22,47–49]; several other changes such as secretion of proteins and chromatic remodeling might contribute to an alternative mechanism of senescence induction [49,50].

GT-induced cell cycle arrest is a phenomenon that has been described in prostate and breast cancer cell lines [20,21]. Previous studies in our laboratory have shown that $p53^{+/+}/p21^{+/+}$ and $p53^{-/-}/p21^{+/+}$ cells undergo S-phase arrest in response to GT, yet at higher concentrations perhaps due to the different source of the drug [19]. In this study, we similarly observed that GT causes an accumulation in the S-phase population with decreased proliferation irrespective of the p53 and p21 status of HCT116 cells [34,51]. One of the most important mediators of p53-dependent cell cycle arrest is the CDKI p21 that has prominent roles in S-phase arrest [45]. Although the absence of p21 and p53 gene in HCT116 cells correlates with increased sensitivity to cell death induction by GT, the fact that HCT116 $p53^{+/+}/p21^{-/-}$ cells also arrested at the S-phase implies that p21 is not the only inducer of this arrest. This observation is consistent with other published data, where p21 expression was not associated with the S-phase arrest action of PGG [20]. Further molecular investigation of cell cycle and mitosis markers revealed that prolonged GT treatment stimulated distinct molecular effects depending on the p21 and p53 presence. In the $p53^{+/+}/p21^{+/+}$ cells, longer GT treatment blocked the cell cycle allowing optimal cell cycle checkpoint activation against the damaging drug GT, that is also displayed by the low amount of multinucleated cells. While prolonged GT treatment in the absence of the key cell cycle regulators p53 and p21 allowed damaged cells to overcome cell cycle block leading to high levels of multinucleated cells in the $p53^{+/+}/p21^{-/-}$ and $p53^{-/-}/p21^{+/+}$ cells. Multinucleated enlarged cell formations are signs of mitotic catastrophe suggesting that GT treatment may also induce this mode of cell death [52]. However, the depletion of mitotic markers has been previously shown to be also associated with senescence [53], thus we can speculate that GT effect can implicate both senescence and mitotic catastrophe as modes of anti-tumor activity. Collectively, these results observed after 48 h of GT treatment in cells lacking p53 and p21 might suggest mitotic catastrophe, or direct entry into senescence from the S or M phases. Whereas in $p53^{+/+}/p21^{+/+}$ cells, senescence is unlikely to occur from M considering the cell cycle blocking effects of GT and is more likely to occur from the S-phase. In fact, previous literature has shown that senescence is a phenomenon that can take place in cells of the S or the M phases of the cell cycle [54].

Senescence induction has been shown to be associated with changes in the metabolism of oxygen radicals [42]. In fact, conditions which induce senescence often appear to be accompanied by a rise in intracellular ROS levels and many studies have validated the link between oxidants and senescence [55,56]. PGG-induced senescence response in breast cancer cells has been found to be mediated by intracellular ROS generation [22]. We observed a dose-dependent increase in ROS generation after GT treatment in HCT116 colon cancer cell lines without much effect on the normal intestinal cells. The lower GT doses of 20 μg/mL, which increased the production of ROS, were found to lead to senescence induction. This increase in ROS production by GT may be due to its ability to alter the levels of the key ROS scavenging antioxidants GSH, SOD and CAT, thus disrupting the redox balance in the cell. We showed that the greatest depletion occurred in the major thiol antioxidant GSH, an important natural defense against oxidative stress [57]. The ability of GT to alter antioxidant enzyme levels in the cell is in accordance with the findings that the tannin compound, epigallocatechin gallate (EGCG), is able to regulate the antioxidant enzymes CAT and SOD differentially in epithelial cells [58]. Similar to EGCG, GT increased the levels of CAT, suggesting that this increase may be part of a defense system designed to eliminate ROS produced by GT. It is interesting to note that pre-treating cells with the thiol containing compounds, NAC a known GSH precursor and DTT reduced the levels of ROS to a larger extent than the enzymatic antioxidants SOD and CAT, suggesting that the former antioxidants may play a more important role in scavenging ROS induced by GT.

We then investigated the role of ROS in GT-induced senescence. Blocking ROS with NAC and DTT attenuated senescence-induced β-galactosidase activity in response to GT but did not block it completely. These results confirm that the senescence induction potential of GT is via ROS production although ROS may not be the sole determinants of GT-induced senescence. The partial uncoupling of ROS in senescence induction was also shown in other models, namely human fibroblasts whereby antioxidant treatment did not prevent drug-induced senescence.

One of the drawbacks of anti-cancer drugs is the relapse of tumors after cessation of treatment. Therefore, it was of concern to determine whether GT effect in HCT116 cells is reversible. GT was shown to significantly reduce colony formation in HCT116 cells especially at concentrations higher than 20 μg/mL GT. HCT116 $p53^{-/-}/p21^{+/+}$ and $p53^{+/+}/p21^{-/-}$ cells were unable to form colonies after GT confirming the higher sensitivity of these cells to the drug. Moreover, GT treatment led to reduced anchorage independent colony formation in soft agar supporting the anti-tumorigenic effect of GT in colon cancer cells. The long-term anti-tumorigenic potential of GT after the cells were released from drug treatment supported its irreversible potential. Such irreversible outcome might be due to drug-induced DNA damage. It has been frequently described that the extent of DNA damage determines cell fate leading to proliferation arrest, senescence, or apoptosis [30,59,60]. Moreover, cellular senescence or apoptosis are known to be triggered by different drug concentrations [61]. Our results describe for the first time the DNA damaging potential of GT in HCT116 cell lines. GT was able to induce the formation of DNA damage foci and the expression of p-H2AX increased proportionally to the concentration of GT used. GT could be a direct-acting compound having a direct effect on DNA damage, since the strong antioxidant NAC failed to completely protect from GT-induced DNA damage. The fact that p-H2AX was induced in all three cell lines indicate that DNA damage by GT occurs in a p53-independent manner which is in accordance with other studies [62]. p-H2AX is linked to a DNA damage response, specifically of double strand breaks, and it has been reported to be responsible for DNA damage repair [62,63]. On the other hand, DNA damage is associated with senescence if H2AX activation occurs at the same GT concentration needed for senescence induction [59]. Indeed, low doses of GT resulted in senescence induction with a perceived amount of DNA damage whereas at high doses extensive DNA damage occurred in the cells leading to apoptosis [19]. Different studies indicate that DNA damage constitutes the primary cause of proliferation arrest and senescence in response to various stimuli. In fact they show that the activation of the DNA damage response is implicated in the establishment of cellular senescence [40,54,63–65]. DNA damage stresses frequently accompany cellular accumulation of ROS, and this cumulative oxidative damage also induces senescence [55,66]. This link between DNA damage and senescence has been demonstrated in several cancer cell lines including colon, ovarian carcinoma cells and breast cancer cells [54,67].

In conclusion, GT was able to induce senescence, ROS generation, and DNA damage in three HCT116 cell lines that are wildtype or knockout for p53 and p21. GT-induced senescence independent of the cellular status of p21 and p53 but the impairment of the p53 axis led to an increased apoptotic cell population by the abolishment of the cell cycle block and further cycling of highly damaged multinucleated cells.

Interestingly, GT is capable of modulating the interconnected matrix of pathways (DNA damage, senescence, ROS, and mitotic catastrophe) that together are capable of driving and restraining tumor development. Understanding the different molecular mechanisms by which GT induces growth inhibition is essential for translating this plant derived compound to the clinic, especially that the broad spectrum of GT effects are not dependent on the p53–p21 pathway which is altered in many tumors. Indeed, p53 mutations are common in more than 70% of colorectal cancer [68,69] adding to the promising effects of GT against colon cancer.

ACKNOWLEDGMENTS

We would like to acknowledge the German Academic Exchange Service, DAAD, for providing Ms. Racha Al-Halabi with funds to support her travel and research stay in Germany. We also thank the Lebanese Research team Funds (ER031) at the Lebanese University for financial support, and the German Deutsche Forschungsgemeinschaft for providing stipend support for Ms. Racha Al-Halabi.

REFERENCES

1. Jemal A, Bray F, Center MM, Ferlay J, Ward E, Forman D. Global cancer statistics. CA Cancer J Clin 2011;61:69–90.
2. Heavey PM, McKenna D, Rowland IR. Colorectal cancer and the relationship between genes and the environment. Nutr Cancer 2004;48:124–141.
3. Chan AT, Giovannucci EL. Primary prevention of colorectal cancer. Gastroenterology 2010;138:2029–2043, e2010.
4. Liu RH. Potential synergy of phytochemicals in cancer prevention: Mechanism of action. J Nutr 2004;134:3479S–3485S.
5. Wolpin BM, Mayer RJ. Systemic treatment of colorectal cancer. Gastroenterology 2008;134:1296–1310.
6. da Rocha AB, Lopes RM, Schwartsmann G. Natural products in anticancer therapy. Curr Opin Pharmacol 2001;1:364–369.
7. Umar A, Viner JL, Richmond E, Anderson WF, Hawk ET. Chemoprevention of colorectal carcinogenesis. Int J Clin Oncol 2002;7:2–26.
8. Ramos S. Cancer chemoprevention and chemotherapy: Dietary polyphenols and signalling pathways. Mol Nutr Food Res 2008;52:507–526.
9. Asensi M, Ortega A, Mena S, Feddi F, Estrela JM. Natural polyphenols in cancer therapy. Crit Rev Clin Lab Sci 2011;48:197–216.
10. Nam S, Smith DM, Dou QP. Tannic acid potently inhibits tumor cell proteasome activity, increases p27 and Bax expression, and induces G1 arrest and apoptosis. Cancer Epidemiol Biomarkers Prev 2001;10:1083–1088.
11. Bawadi HA, Bansode RR, Trappey A II, Truax RE, Losso JN. Inhibition of Caco-2 colon, MCF-7 and Hs578T breast, and DU 145 prostatic cancer cell proliferation by water-soluble black bean condensed tannins. Cancer Lett 2005;218:153–162.
12. Araujo JR, Goncalves P, Martel F. Chemopreventive effect of dietary polyphenols in colorectal cancer cell lines. Nutr Res 2011;31:77–87.
13. Lambert JD, Yang CS. Mechanisms of cancer prevention by tea constituents. J Nutr 2003;133:3262S–3267S.
14. Rudolf E, Andelova H, Cervinka M. Polyphenolic compounds in chemoprevention of colon cancer—Targets and signaling pathways. Anticancer Agents Med Chem 2007;7:559–575.
15. Blenn C, Wyrsch P, Althaus FR. The ups and downs of tannins as inhibitors of poly(ADP-ribose)glycohydrolase. Molecules 2011;16:1854–1877.
16. Feldman KS, Sahasrabudhe K, Lawlor MD, Wilson SL, Lang CH, Scheuchenzuber WJ. In vitro and in vivo inhibition of LPS-stimulated tumor necrosis factor-alpha secretion by the gallotannin beta-D-pentagalloylglucose. Bioorg Med Chem Lett 2001;11:1813–1815.
17. Lee SJ, Lee IS, Mar W. Inhibition of inducible nitric oxide synthase and cyclooxygenase-2 activity by 1,2,3,4,6-penta-*O*-galloyl-beta-D-glucose in murine macrophage cells. Arch Pharm Res 2003;26:832–839.
18. Erdelyi K, Kiss A, Bakondi E, et al. Gallotannin inhibits the expression of chemokines and inflammatory cytokines in A549 cells. Mol Pharmacol 2005;68:895–904.
19. Al-Ayyoubi S, Gali-Muhtasib H. Differential apoptosis by gallotannin in human colon cancer cells with distinct p53 status. Mol Carcinog 2007;46:176–186.
20. Chai Y, Lee HJ, Shaik AA, et al. Penta-*O*-galloyl-beta-D-glucose induces G1 arrest and DNA replicative S-phase arrest independently of cyclin-dependent kinase inhibitor 1A, cyclin-dependent kinase inhibitor 1B and P53 in human breast cancer cells and is orally active against triple negative xenograft growth. Breast Cancer Res 2010;12:R67.
21. Hu H, Zhang J, Lee HJ, Kim SH, Lu J. Penta-*O*-galloyl-beta-D-glucose induces S- and G(1)-cell cycle arrests in prostate cancer cells targeting DNA replication and cyclin D1. Carcinogenesis 2009;30:818–823.
22. Yin S, Dong Y, Li J, Lu J, Hu H. Penta-1,2,3,4,6-*O*-galloyl-beta-D-glucose induces senescence-like terminal S-phase arrest in human hepatoma and breast cancer cells. Mol Carcinog 2011;50:592–600.
23. Gali-Muhtasib HU, Younes IH, Karchesy JJ, el-Sabban ME. Plant tannins inhibit the induction of aberrant crypt foci and colonic tumors by 1,2-dimethylhydrazine in mice. Nutr Cancer 2001;39:108–116.
24. Al-Halabi R, Bou Chedid M, Abou Merhi R, et al. Gallotannin inhibits NFkB signaling and growth of human colon cancer xenografts. Cancer Biol Ther 2011;12:59–68.
25. Mathon NF, Lloyd AC. Cell senescence and cancer. Nat Rev Cancer 2001;1:203–213.
26. Campisi J, d'Adda di Fagagna F. Cellular senescence: When bad things happen to good cells. Nat Rev Mol Cell Biol 2007;8:729–740.
27. Ben-Porath I, Weinberg RA. The signals and pathways activating cellular senescence. Int J Biochem Cell Biol 2005;37:961–976.
28. Kuilman T, Michaloglou C, Mooi WJ, Peeper DS. The essence of senescence. Genes Dev 2010;24:2463–2479.
29. Downey M, Durocher D. Chromatin and DNA repair: The benefits of relaxation. Nat Cell Biol 2006;8:9–10.
30. Gordon RR, Nelson PS. Cellular senescence and cancer chemotherapy resistance. Drug Resist Updat 2012;15:123–131.
31. Acosta JC, Gil J. Senescence: A new weapon for cancer therapy. Trends Cell Biol 2012;22:211–219.
32. Munshi A, Hobbs M, Meyn RE. Clonogenic cell survival assay. Methods Mol Med 2005;110:21–28.
33. Ke N, Wang X, Xu X, Abassi YA. The xCELLigence system for real-time and label-free monitoring of cell viability. Methods Mol Biol 2011;740:33–43.
34. Irelan JT, Wu MJ, Morgan J, et al. Rapid and quantitative assessment of cell quality, identity, and functionality for cell-based assays using real-time cellular analysis. J Biomol Screen 2011;16:313–322.
35. Abassi YA, Xi B, Zhang W, et al. Kinetic cell-based morphological screening: Prediction of mechanism of compound action and off-target effects. Chem Biol 2009;16:712–723.
36. Thant AA, Wu Y, Lee J, et al. Role of caspases in 5-FU and selenium-induced growth inhibition of colorectal cancer cells. Anticancer Res 2008;28:3579–3592.
37. Pan D, Marcato P, Ahn DG, et al. Activation of p53 by chemotherapeutic agents enhances reovirus oncolysis. PLoS ONE 2013;8:e54006.
38. Narita M. Cellular senescence and chromatin organisation. Br J Cancer 2007;96:686–691.
39. Kosar M, Bartkova J, Hubackova S, Hodny Z, Lukas J, Bartek J. Senescence-associated heterochromatin foci are dispensable for cellular senescence, occur in a cell type- and insult-dependent manner and follow expression of p16(ink4a). Cell Cycle 2011;10:457–468.
40. Di Micco R, Sulli G, Dobreva M, et al. Interplay between oncogene-induced DNA damage response and heterochromatin in senescence and cancer. Nat Cell Biol 2011;13:292–302.
41. Acharya A, Das I, Chandhok D, Saha T. Redox regulation in cancer: A double-edged sword with therapeutic potential. Oxid Med Cell Longev 2010;3:23–34.
42. Lu T, Finkel T. Free radicals and senescence. Exp Cell Res 2008;314:1918–1922.
43. Passos JF, Saretzki G, von Zglinicki T. DNA damage in telomeres and mitochondria during cellular senescence: Is there a connection? Nucleic Acids Res 2007;35:7505–7513.
44. Saretzki G. Cellular senescence in the development and treatment of cancer. Curr Pharm Des 2010;16:79–100.
45. Abbas T, Dutta A. p21 in cancer: Intricate networks and multiple activities. Nat Rev Cancer 2009;9:400–414.
46. Soria G, Gottifredi V. PCNA-coupled p21 degradation after DNA damage: The exception that confirms the rule? DNA Repair (Amst) 2010;9:358–364.

47. Chang BD, Swift ME, Shen M, Fang J, Broude EV, Roninson IB. Molecular determinants of terminal growth arrest induced in tumor cells by a chemotherapeutic agent. Proc Natl Acad Sci USA 2002;99:389–394.
48. Medcalf AS, Klein-Szanto AJ, Cristofalo VJ. Expression of p21 is not required for senescence of human fibroblasts. Cancer Res 1996;56:4582–4585.
49. Prieur A, Besnard E, Babled A, Lemaitre JM. p53 and p16(INK4A) independent induction of senescence by chromatin-dependent alteration of S-phase progression. Nat Commun 2011;2:473.
50. Passos JF, Simillion C, Hallinan J, Wipat A, von Zglinicki T. Cellular senescence: Unravelling complexity. Age (Dordr) 2009;31:353–363.
51. Weiland T, Berger A, Essmann F, Lauer UM, Bitzer M, Venturelli S. Kinetic tracking of therapy-induced senescence using the real-time cell analyzer single plate system. Assay Drug Dev Technol 2012;10:289–295.
52. Roninson IB, Broude EV, Chang BD. If not apoptosis, then what? Treatment-induced senescence and mitotic catastrophe in tumor cells. Drug Resist Updat 2001;4:303–313.
53. Eom YW, Kim MA, Park SS, et al. Two distinct modes of cell death induced by doxorubicin: Apoptosis and cell death through mitotic catastrophe accompanied by senescence-like phenotype. Oncogene 2005;24:4765–4777.
54. te Poele RH, Okorokov AL, Jardine L, Cummings J, Joel SP. DNA damage is able to induce senescence in tumor cells in vitro and in vivo. Cancer Res 2002;62:1876–1883.
55. Passos JF, Von Zglinicki T. Oxygen free radicals in cell senescence: Are they signal transducers? Free Radic Res 2006;40:1277–1283.
56. Macip S, Igarashi M, Fang L, et al. Inhibition of p21-mediated ROS accumulation can rescue p21-induced senescence. EMBO J 2002;21:2180–2188.
57. Pelicano H, Carney D, Huang P. ROS stress in cancer cells and therapeutic implications. Drug Resist Updat 2004;7:97–110.
58. Yamamoto T, Hsu S, Lewis J, et al. Green tea polyphenol causes differential oxidative environments in tumor versus normal epithelial cells. J Pharmacol Exp Ther 2003;307:230–236.
59. Rebbaa A, Zheng X, Chu F, Mirkin BL. The role of histone acetylation versus DNA damage in drug-induced senescence and apoptosis. Cell Death Differ 2006;13:1960–1967.
60. d'Adda di Fagagna F. Living on a break: Cellular senescence as a DNA-damage response. Nat Rev Cancer 2008;8:512–522.
61. Costantino VV, Mansilla SF, Speroni J, et al. The sesquiterpene lactone dehydroleucodine triggers senescence and apoptosis in association with accumulation of DNA damage markers. PLoS ONE 2013;8:e53168.
62. Chiu SJ, Lee YJ, Hsu TS, Chen WS. Oxaliplatin-induced gamma-H2AX activation via both p53-dependent and -independent pathways but is not associated with cell cycle arrest in human colorectal cancer cells. Chem Biol Interact 2009;182:173–182.
63. Podhorecka M, Skladanowski A, Bozko P. H2AX phosphorylation: Its role in DNA damage response and cancer therapy. J Nucleic Acids 2010;2010:920161.
64. Bartkova J, Rezaei N, Liontos M, et al. Oncogene-induced senescence is part of the tumorigenesis barrier imposed by DNA damage checkpoints. Nature 2006;444:633–6637.
65. Rodier F, Coppe JP, Patil CK, et al. Persistent DNA damage signalling triggers senescence-associated inflammatory cytokine secretion. Nat Cell Biol 2009;11:973–979.
66. Lleonart ME, Artero-Castro A, Kondoh H. Senescence induction; a possible cancer therapy. Mol Cancer 2009;8:3.
67. Song YS, Lee BY, Hwang ES. Dinstinct ROS and biochemical profiles in cells undergoing DNA damage-induced senescence and apoptosis. Mech Ageing Dev 2005;126:580–590.
68. Smith G, Carey FA, Beattie J, et al. Mutations in APC, Kirsten-ras, and p53–alternative genetic pathways to colorectal cancer. Proc Natl Acad Sci USA 2002;99:9433–9438.
69. Shen L, Toyota M, Kondo Y, et al. Integrated genetic and epigenetic analysis identifies three different subclasses of colon cancer. Proc Natl Acad Sci USA 2007;104:18654–18659.

SUPPORTING INFORMATION

Additional supporting information may be found in the online version of this article at the publisher's web-site.